Liquid Crystals
Publication details, including instructions for authors and subscription information:
http://www.informaworld.com/smpp/title~content=t713926090

Structure-activity studies of ferroelectric and antiferroelectric imine ligands and their square-planar complexes

R. Piñol[a]; M. B. Ros[a]; J. L. Serrano Corresponding author[a]; T. Sierra[a]; M. R. De La Fuente[b]
[a] Química Orgánica, Facultad de Ciencias-I.C.M.A, Universidad de Zaragoza-C.S.I.C., 50009-Zaragoza, Spain [b] Dept. Física Aplicada II, Facultad de Ciencias, Universidad del País Vasco, 48080-Bilbao, Spain

Online publication date: 21 May 2010

To cite this Article Piñol, R. , Ros, M. B. , Serrano Corresponding author, J. L. , Sierra, T. and De La Fuente, M. R.(2004) 'Structure-activity studies of ferroelectric and antiferroelectric imine ligands and their square-planar complexes', Liquid Crystals, 31: 9, 1293 — 1303
To link to this Article: DOI: 10.1080/02678290412331284521
URL: http://dx.doi.org/10.1080/02678290412331284521

LIQUID CRYSTALS, VOL. 31, NO. 9, SEPTEMBER 2004, 1293–1303

Structure–activity studies of ferroelectric and antiferroelectric imine ligands and their square-planar complexes

R. PIÑOL, M. B. ROS, J. L. SERRANO*, T. SIERRA

Química Orgánica, Facultad de Ciencias-I.C.M.A., Universidad de Zaragoza-C.S.I.C., 50009-Zaragoza, Spain

and M. R. DE LA FUENTE

Dept. Física Aplicada II, Facultad de Ciencias, Universidad del País Vasco, Aptdo. 644, 48080-Bilbao, Spain

(*Received 9 March 2004; accepted 11 May 2004*)

The synthesis and characterization of the mesomorphic and dielectric properties of a series of new imine-based liquid crystalline compounds that exhibit tilted SmC* phases is reported. The presence of an imino linkage within the mesogenic nucleus of these compounds is significant due to the ability of salicylaldimines to coordinate to metals. Structure–activity studies have also been carried out by varying the structural elements in the ligands. The structural variations include changing the length of the chiral chain and incorporating fluorocarbon segments in the achiral terminal chain.

1. Introduction

The appearance of ferroelectric and/or antiferroelectric liquid crystal behaviour in Schiff's bases and their corresponding palladium(II) complexes has been shown to depend on subtle structural changes [1]. For instance, the significant role of the intramolecular orientation of dipoles associated with the core linkages has been demonstrated. Moreover, the coordinating properties of Schiff's bases [2], which allow the formation of dimeric complexes with antiparallel orientation of the rod-like ligands within a square planar structure, has led to a metallomesogen with a broad antiferroelectric mesophase. This type of antiferroelectric liquid crystalline material had no precedent in the literature.

We considered it of interest to investigate some structural modifications that would allow a greater understanding of the relationships between the structure and the appearance of antiferroelectric and/or ferroelectric properties in chiral imine-derived organic ligands and their square-planar metal complexes. On the basis of literature reports and as a continuation of previous studies, we carried out two types of structural modification: (i) the optical activity of the molecule was altered by increasing the length of the chiral chain to incorporate an odd or even number of carbon atoms [**L1(H,7)**, **L1(H,14)**, **L2(F,7)**, **L2(F,14)**, in scheme 1], and (ii) the achiral chain was changed by introducing fluorocarbon segments to induce microsegregation phenomena and hence influence the stabilization of mesomorphism (**L1** series vs. **L2** series, in scheme 1). The first structural change is known to be the origin of an odd–even effect that strongly affects antiferroelectric behaviour in biphenyl-ester derivatives [3, 4]. The second change has been reported as a means to stabilize the ferroelectric SmC* mesophase [5, 6].

L1(H,n)

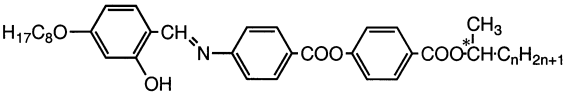

n = 6 **L1(H,6)**

n = 7 **L1(H,7)**

n = 14 **L1(H,14)**

L2(F,n)

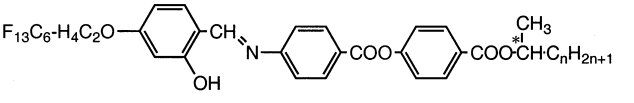

n = 6 **L2(F,6)**

n = 7 **L2(F,7)**

n = 14 **L2(F,14)**

Scheme 1. Structures of ligands.

*Author for correspondence; e-mail: joseluis@unizar.es

Liquid Crystals ISSN 0267-8292 print/ISSN 1366-5855 online © 2004 Taylor & Francis Ltd
http://www.tandf.co.uk/journals
DOI: 10.1080/02678290412331284521

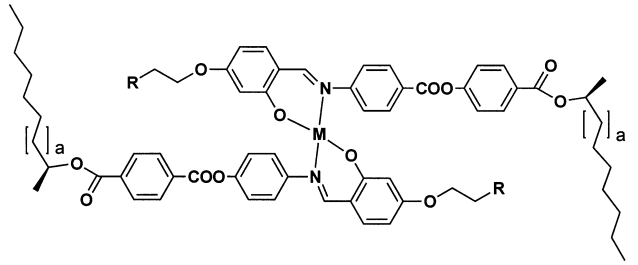

M=Cu; a=0; R=C_6H_{13} **L1(H,6)-Cu**
M=VO; a=0; R=C_6H_{13} **L1(H,6)-VO**
M=VO; a=1; R=C_6H_{13} **L1(H,7)-VO**
M=VO; a=1; R=C_6F_{13} **L2(F,7)-VO**

Scheme 2. Structures of complexes.

The work described here deals with the synthesis and characterization (liquid crystal and dielectric) of different salicylaldimine derivatives (scheme 1). All of these ligands consist of a three-ring mesogenic core in which the aromatic rings are linked by two different groups, namely an imino and an ester group—the former has rarely been employed in the design of antiferroelectric liquid crystals [7]. Furthermore, these Schiff's bases have the ability to coordinate to a variety of metals, for example, vanadium(IV), copper(II), palladium(II), through chelation of the N (imine) and O (hydroxyl group) heteroatoms. This process enables the formation of dimeric complexes in which the two ligands are oriented antiparallel with respect to each other within a planar geometry (scheme 2).

All of the compounds were studied by optical microscopy, DSC and dielectric spectroscopy. Spontaneous polarization values were evaluated by the triangular wave method [8] where possible.

2. Results and discussion

2.1. *Study of the ligands*

2.1.1. *Synthesis*

The synthetic route used to prepare the ligands is shown in scheme 3. The final step is, in all cases, the condensation of the aniline and the corresponding aldehyde to form the imine linkage.

(*R*)-2-Octanol, (*R*)-2-nonanol and (*R*)-2-hexadecanol are the chiral chains chosen for this study. (*R*)-2-Octanol is commercially available from Aldrich; (*R*)-2-nonanol and (*R*)-2-hexadecanol were obtained from their corresponding commercial racemic mixtures by enzymatic acetylation. The enantiomeric resolution was carried out with Lipase, Type II, from porcine pancreas, a compound that catalyses the enantioselective acetylation of the *R*-enantiomer of the alcohol over the *S*-enantiomer. Optimal conditions were found to be as follows: 4/1 molar excess of vinyl acetate with diisopropyl ether as solvent at room temperature. The enantiomeric excess was determined by chiral gas chromatography of the acetate derivatives.

The aforementioned chiral chains were coupled with benzyl-protected 4-hydroxybenzoic acid. Dicyclohexylcarbodiimide was found to be the most appropriate esterification agent for 2-octanol and 2-nonanol but did not promote the reaction with 2-hexadecanol. The Mitsunobu method [9] was used in the latter case and gave rise to the *S*-configuration in the stereogenic centre after reaction with the acid. The chiral phenols were coupled with *p*-nitrobenzoic acid (the nitro group was subsequently reduced to amino [1]) to yield the corresponding chiral moieties for the final ligands. These chiral moieties were coupled with the corresponding 2-hydroxy-4-alkoxybenzaldehyde in ethanol with acetic acid as a catalyst. These reactions gave the target Schiff's bases. The synthetic conditions for the preparation of the 2-hydroxy-4-alkoxybenzaldehyde depended upon the nature of the chain. Williamson conditions were used for hydrocarbon chains, while the Mitsunobu method was used to incorporate 1*H*,1*H*,2*H*,2*H*-perfluorooctanol. Attempts to use the Williamson method with 1*H*,1*H*,2*H*,2*H*-perfluorooctyliodide led to potassium bicarbonate-promoted intramolecular elimination of HI instead of coupling to the phenol [10].

2.1.2. *Mesomorphic properties*

The thermal properties of the ligands were investigated by polarizing optical microscopy (POM) and differential scanning calorimetry (DSC). The results are given in the table. All the ligands prepared show mesomorphic behaviour over a wide temperature range. Moreover, they all show the potentially ferroelectric SmC* mesophase. An antiferroelectric mesophase was identified by observation of textures through POM for **L1(H,6)**. The change to antiferroelectric ordering in the tilted smectic mesophase was particularly clear. Dechiralization lines were visible over the whole ferroelectric range but disappeared on reaching the antiferroelectric ordering. This phenomenon was further confirmed by dielectric spectroscopy studies [1].

As mentioned already, two molecular characteristics are considered here in terms of their influence on the mesomorphic behaviour: (i) changes in the optical activity of the molecule by increasing the length of the chiral chain and incorporating an odd or even number of carbon atoms, and (ii) the effect of the presence of fluorocarbon segments in the achiral chain versus hydrocarbon chains. The consequences of these structural changes are represented in figure 1.

An increase in the chirality of the molecules by

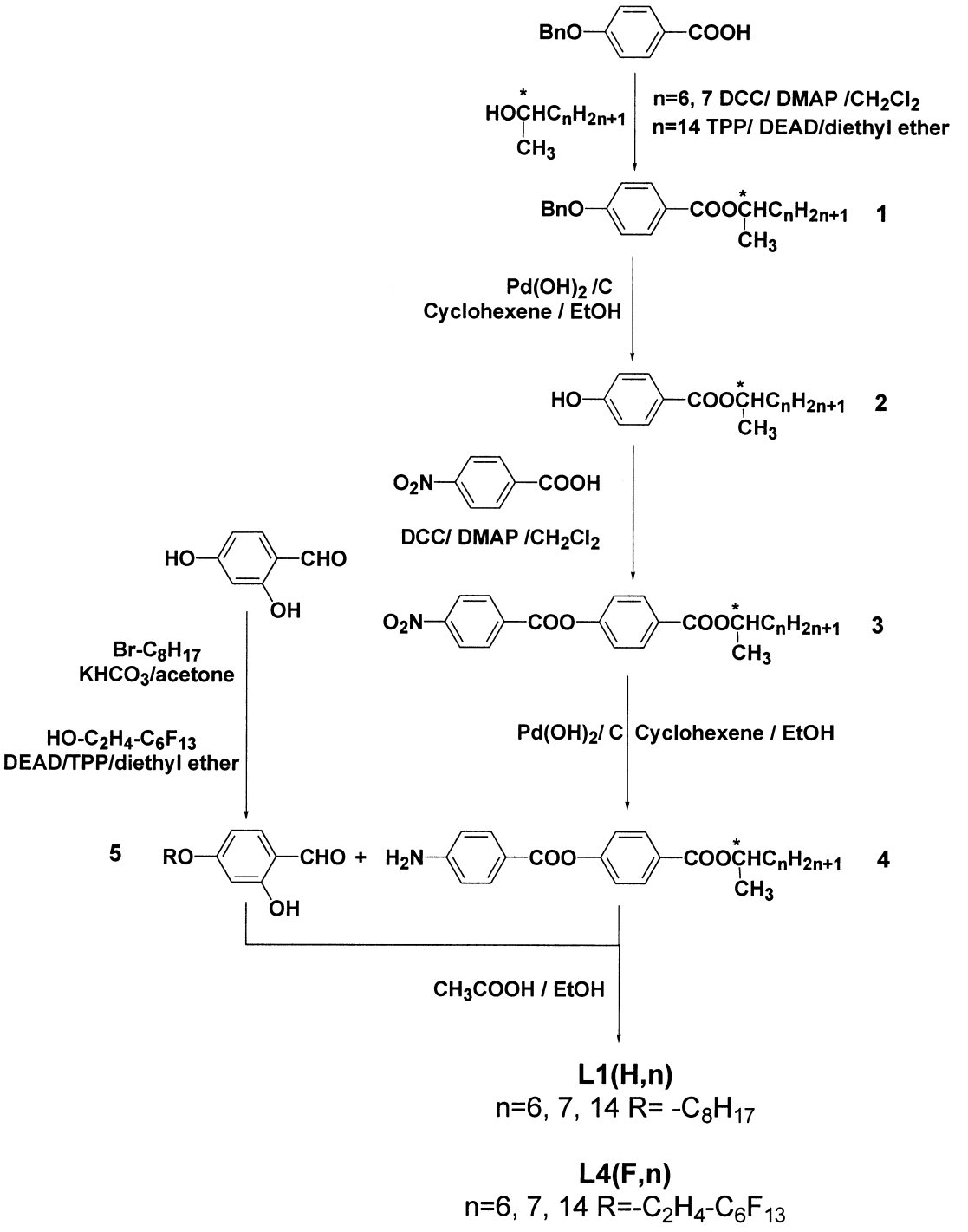

Scheme 3. Synthesis of ligands.

lengthening the alkyl group in the stereogenic centre led to significant changes in the mesomorphic behaviour. On changing from an even number of carbon atoms in this alkyl group, **L1(H,6)**, to an odd number, **L1(H,7)**, the polymorphism of the SmC* mesophase disappeared while the mesophase temperature range remained the same. Indeed, the whole mesomorphic range below the SmA mesophase is occupied by a ferroelectric SmC* mesophase in the modified compound and the antiferroelectric ordering disappeared. This is in agreement with results found by several authors on biphenyl-ester derivatives [3, 4]. A very long alkyl group, **L1(H,14)**, destabilizes SmC* ordering (which only appears during

Table. Thermal and thermodynamic properties of the ligands and their complexes.

Compound	Transition temperatures /°C [transition enthalpies ΔH/KJ mol^{-1}]
L1(H,6)	Cr 108[32.5] SmC$^*_A$ 112[a] SmC* 139[a] SmA 173[4.5] I
L1(H,7)	Cr 110.6[38.4] SmC* 139.1[0.4] SmA 172.6[4.8] I
L1(H,14)	Cr 96.2[36.8] (SmC* 86.4[0.7]) SmA 131.6[2.7] I
L2(F,6)	Cr 160[48.3] SmC* 178.7[0.8] SmA 223[4.9] I
L2(F,7)	Cr 155.8[41.0] SmC* 178.3[0.7] SmA 222.8[4.1] I
L2(F,14)	Cr 145.5[44.2] (SmC* 140.4[0.4]) SmA 187.8[3.1] I
L1(H,6)-Pd[d]	Cr 225 [59.7] SmA 270 dec
L1(H,6)-Cu	Cr 198[25.2] SmC* 215 [0.4] SmA 245 [6.8] I
L1(H,6)-VO	Cr 172[12.3] SmC* 189[a] SmA 230 I[b]
L1(H,7)-VO	Cr 177[12.6] SmC* 190[a] SmA 249 I
L2(F,7)-VO	Cr 136[19.9] Sm[e] 173[18.0] SmC* 236[9.7] SmA – I[b,c]

[a]Transition temperatures taken from optical microscopy observations.
[b]Some decomposition is observed during the transition to the isotropic state.
[c]The transitions SmC*–SmA and SmA–I appear overlapped in the DSC scan. The temperature corresponds to the peak maximum.
[d]See ref. [1].
[e]Unidentified highly ordered Sm mesophase.

the cooling process) and this change is associated with a sharp decrease in the clearing point. The same trend is observed in the series of fluorinated derivatives, **L2(F,*n*)**.

A significant increase in the melting and clearing temperatures is observed when fluorocarbon segments are included in the achiral terminal chain. The general behaviour of fluorinated compounds—in comparison with the corresponding hydrocarbon analogues—is characterized by wider temperature ranges of the orthogonal SmA mesophase along with shorter ferroelectric mesophase ranges. It has been reported that fluorocarbon terminal chains stabilize smectic mesomorphism [11]. Moreover, it has also been observed that the appearance of the SmC mesophase is very dependent on the length of the fluorocarbon segment and the relationship between the size of fluorocarbon and hydrocarbon segments. This dependence varies with the structure of the mesogenic core. Indeed, if a high degree of fluorination favours the SmC mesophase in phenyl benzoate liquid crystals [6], an unexpected destabilization of the ferroelectric mesophase has been reported for benzaldimine derivatives [5]. A similar trend was also observed for the antiferroelectric mesophase [12, 13]. In the particular case described here, the antiferroelectric SmC$^*_A$ phase does not appear in any of the compounds bearing fluorocarbon chains—a fact confirmed by dielectric studies.

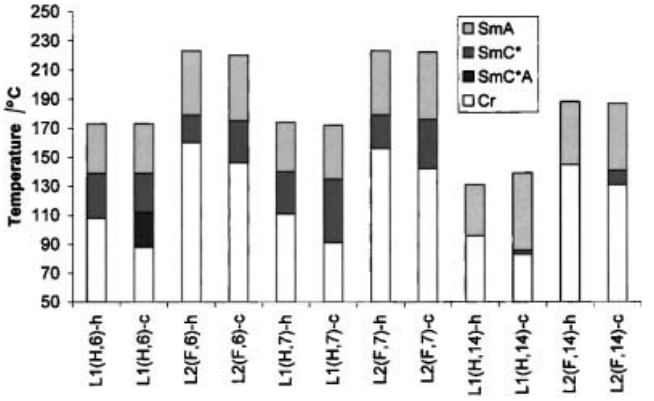

Figure 1. Transitional behaviour of the ligands on heating (h) and cooling (c).

2.1.3. *Ferroelectric properties of the ligands*

All the ligands that show the SmC* mesophase were studied under the influence of an alternating electric field in 5 μm cells with a polyimide coating (to achieve homogeneous alignment) and inner ITO electrodes. The spontaneous polarization was measured for the hydrocarbon compounds **L1(H,6)** and **L1(H,7)**. The maximum value reached in both cases was around 80 nC cm^{-2}, which demonstrates a negligible influence on the ferroelectric behaviour of the odd–even effect associated with the chiral chain. This value is close to those reported for structurally analogous FLCs consisting of a three-ring mesogenic core and an alkoxycarbonyl chiral tail [3, 14]. All of the measurements were made at 8.5 V_{pp} μm^{-1} and 50 Hz. The ferroelectric nature of the SmC* mesophase of these compounds was confirmed by the appearance of large Goldstone modes (250 and 60, respectively) in the dielectric measurements.

Unfortunately, polarization values could not be accurately determined for fluorocarbon derivatives **L2(F,6)** and **L2(F,7)** due to the appearance, during the application of an external electric field, of air bubbles within the ITO cells. This contrasts with results reported for other fluorocarbon FLCs, which do not contain the imine linkage group [6*a*, 12]. Indeed, high $\mathbf{P}_s$ values have been measured for phenyl 4-benzoyloxybenzoate derivatives that are greater than those measured for their hydrocarbon analogues [12]. Nevertheless, the ferroelectric behaviour of our compounds was confirmed by dielectric measurements. The

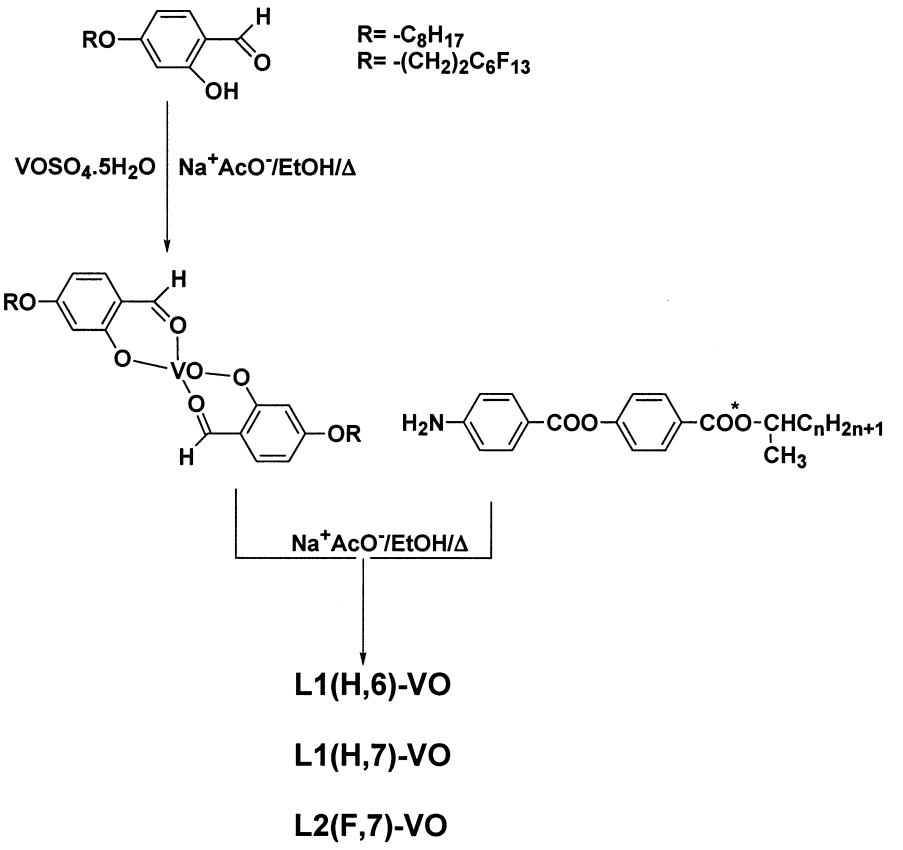

Scheme 4. Synthesis of complexes.

low frequency permittivity (125 Hz) experiences a huge increase at the SmA–SmC* phase transition, a situation that can be attributed to the helix-related ferroelectric Goldstone mode (*c*. 200).

2.2. *Study of the complexes*

Oxovanadium(IV) complexes were prepared for **L1(H,6)**, **L1(H,7)** and **L2(F,7)**. Problems were encountered in the purification of some of these materials and it proved impossible to obtain a pure vanadium(IV) complex of **L2(F,6)**; this compound has therefore been excluded from this study. Palladium(II) [1], copper(II) and vanadium(IV) were previously coordinated to the ligand **L1(H,6)** in order to gain an insight into the mesomorphic behaviour of the three types of complex. The study of the mesomorphic and dielectric behaviour was found to be more reproducible when dealing with oxovanadium complexes. The copper(II) complex, **L1(H,6)-Cu**, gave significant conductivity under an electric field, a phenomenon that masks the actual dielectric behaviour of the compound and prevents reliable measurements of the $\mathbf{P}_s$ value and the permittivity. Due to the low tendency of the longest ligands **L1(H,14)** and **L2(F,14)** to promote mesomorphism, these compounds were not considered in our study.

2.2.1. *Synthesis of the complexes*

The oxovanadium(IV) complexes of the corresponding salicylaldimine ligands, **L1(H,6)**, **L1(H,7)** and **L2(F,7)**, were synthesized in two steps (scheme 4). Firstly, it was necessary to synthesize the complex of the aldehyde intermediate. This reaction was followed by condensation of the complexed carbonyl groups with the corresponding chiral anilines. The formation of the complexes in the reaction of the imine ligand with the metal salt proved to be unfeasible since quantitative complexation did not occur and the remaining ligand could not be separated from the final complex. The copper(II) complex **L1(H,6)-Cu** was synthesized from the corresponding ligand **L1(H,6)** and copper(II) acetate according to the method previously described for the analogous palladium(II) complex [1].

2.2.2. *Mesomorphic behaviour*

The transition temperatures and enthalpies of the complexes are gathered in the table.

The usual fan-shaped and homeotropic textures were

observed for the SmA mesophase of the complexes, which on cooling to the SmC* mesophase changed to give a broken fan-shaped and pseudohomeotropic textures characteristic of the SmC* phase. Only **L1(H,6)-VO** showed fluctuations of the pseudohomeotropic texture of the SmC* prior to crystallization, indicating possible antiferroelectric ordering.

The structural modifications made to the ligands were found significantly to influence the mesomorphic behaviour of the complexes. Increasing the length of the chiral chain by a methylene group, **L1(H,6)-VO** vs **L1(H,7)-VO**, gave rise to an increase in the SmA temperature range, while the ferroelectric mesophase exists over a similar temperature range in both complexes. No indication of antiferroelectric ordering was observed in the latter case. However, the most surprising effect concerns the incorporation of a perfluorinated segment in the achiral tail of the ligand. In contrast to the situation observed on comparing the ligands **L1(H,7)** and **L2(F,7)**, the presence of partially fluorinated chains enhances the ferroelectric layered order in the complex **L2(F,7)-VO** at the expense of the orthogonal layered SmA phase, (present in **L1(H,7)-VO**), which is almost undetectable in the fluorinated complex.

2.2.3. *Ferroelectric properties of the complexes*

The maximum spontaneous polarization values were measured for some of the complexes displaying an enantiotropic SmC* phase; these are: **L1(H,7)-VO** ($36\,nC\,cm^{-2}$) and **L2(F,7)-VO** ($100\,nC\,cm^{-2}$). The measurements were made with voltages of $10\,V_{pp}\,\mu m^{-1}$ and a frequency of 50 Hz. The value measured for **L1(H,7)-VO** is similar to those of related Schiff's base oxovanadium complexes reported by our group [15]. However, the highest P_s value was measured for the complex **L2(F,7)-VO**, which shows a wide SmC* phase range. This is in accord with results reported in the literature for organic compounds in which an enhancement of the spontaneous polarization occurs with an increase of the fluorination extent in the peripheral chains [6, 12]. The dependence of the dielectric permittivity at low frequency (65 Hz) upon temperature for this complex is shown in figure 2. The plot shows a large Goldstone mode (which is indicative of ferroelectric behaviour) just below the isotropic liquid, thus confirming the absence of the SmA phase present in the ligand. A transition to an unidentified smectic mesophase (SmX) is observed at 160°C, as evidenced by a dramatic decrease in the dielectric permittivity, which does not reflect antiferroelectric behaviour. This phase change is also in accord with DSC studies.

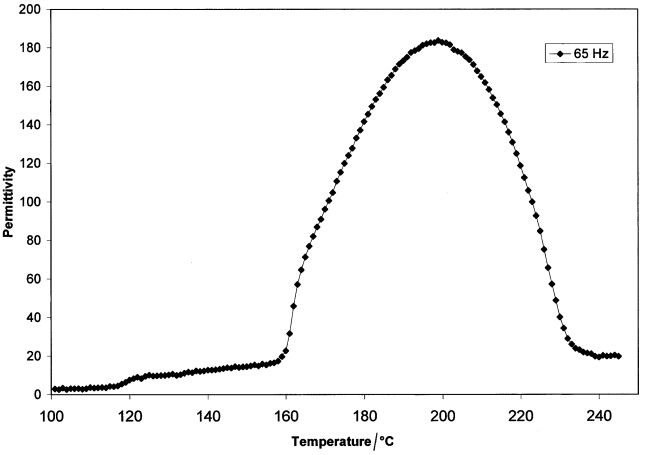

Figure 2. Plot of dielectric permittivity against temperature measured at 65 Hz on cooling for complex **L2(F,7)-VO**.

3. Experimental

3.1. *Synthesis*

3.1.1. *Synthesis of the (1R)-1-methylalkyl acetate*

A mixture of 20.4 mmol of racemic alcohol, 81.6 mmol of vinyl acetate and 2.7 g of porcine pancreatic lipase (PPL) in 45 ml of dry isopropyl ether was stirred at room temperature under an inert atmosphere for 3 days. The mixture was filtered through a pad of Celite® and the solvent was removed under reduced pressure. The crude product was purified by flash chromatography on silica gel using a mixture of hexane/dichloromethane (3/1) as eluant.

3.1.1.1. *(1R)-1-Methyloctyl acetate.* Yield 30% of a yellow oil, ee 93.6%. R_f 0.67 (dichloromethane). ^{1}H NMR (300 MHz, $CDCl_3$): ∂ 0.85 (t, $J=6.6$ Hz, 3H), 1.17 (d, $J=6.2$ Hz, 3H), 1.24 (m, 10H), 1.35–1.49 (m, 1H) 1.50–1.61 (m, 1H), 2.0 (s, 3H), 4.86 (m, 1H).^{13}C NMR (300 MHz, $CDCl_3$): ∂ 14.0, 19.9, 21.3, 22.6, 25.4, 29.2, 29.4, 31.7, 35.9, 71.0, 170.7. IR (Nujol): ν 1738, $1243\,cm^{-1}$. [α] −1.99 ($CHCl_3$) 28°C.

3.1.1.2. *(1R)-1-Methylpentadecyl acetate.* Yield 26% of a yellow oil, ee 98%, R_f 0.74 (dichloromethane). ^{1}H NMR (300 MHz, $CDCl_3$): ∂ 0.86 (t, $J=6.6$ Hz, 3H), 1.18 (d, $J=6.2$ Hz, 3H) 1.23 (m, 24H), 1.35–1.48 (m, 1H) 1.49–1.60 (m, 1H), 2.0 (s, 3H), 4.86 (m, 1H).^{13}C NMR (300 MHz, $CDCl_3$): ∂ 14.1, 19.9, 21.4, 22.7, 25.4, 21.2, 29.3, 29.4, 29.5, 29.6, 31.9, 35.9, 71.0, 170.7. IR (Nujol): ν 1739, $1244\,cm^{-1}$. [α] −0.71 ($CHCl_3$) 27°C.

3.1.2. *Synthesis of the (1R)-1-methylalkylalcohols*

A mixture of 29.2 mmol of pure enantiomeric acetate (*R*-configuration), 36.5 mmol of sodium hydroxide and 40 ml of methanol was heated at reflux for 1 h. Once the mixture had regained room temperature, it was neutralized with

aqueous hydrochloric acid (2M) and the solvent was evaporated. Water was added to the residue and it was extracted several times with diethyl ether. The combined organic layers were washed with saturated aqueous sodium bicarbonate solution, dried over magnesium sulphate and the solvent was removed under reduced pressure. The crude product was purified by flash chromatography using dichloromethane as eluent.

3.1.2.1. *(1R)-1-Methyloctanol.* Yield 90% of a yellow oil, R_f 0.23 (dichloromethane). ^{1}H NMR (300 MHz, $CDCl_3$): ∂ 0.84 (t, $J=6.9$ Hz, 3H), 1.14 (d, $J=6.3$ Hz, 3H), 1.24 (m, 10H), 1.3–1.5 (m, 2H), 3.75 (m, 1H). ^{13}C NMR (300 MHz, $CDCl_3$): ∂ 14.0, 22.6, 23.4, 25.7, 29.2, 29.6, 31.8, 39.3, 68.1. IR (Nujol): ν 3338 (w), 1108 cm^{-1}. [α] −7.37 ($CHCl_3$) 27°C.

3.1.2.2. *(1R)-1-Methylpentadecanol.* Yield 88% of a white solid, m.p. 46°C, R_f 0.30 (dichloromethane). ^{1}H NMR (300 MHz, $CDCl_3$): ∂ 0.84 (t, $J=6.6$ Hz, 3H), 1.15 (d, $J=6.3$ Hz, 3H), 1.22 (m, 24H), 1.32–1.46 (m, 2H), 3.74 (m, 1H). ^{13}C NMR (300 MHz, $CDCl_3$): ∂ 14.0, 22.7, 23.4, 25.7, 29.3, 29.6, 31.9, 39.3, 66.1. IR (Nujol): ν 3283 (w), 1121 cm^{-1}. [α] −4.23 ($CHCl_3$) 27°C.

3.1.3. *General procedure for synthesis of 1-methylalkyl 4-benzyloxybenzoates,* ***1 (n=6,7)***

To a solution of 15 mmol of (2*R*)-2-alkylalcohol in 150 ml of distilled dichloromethane were added 15 mmol of 4-benzyloxybenzoic acid and 1.5 mmol of dimethylaminopyridine (DMAP) under an argon atmosphere. The mixture was cooled in an ice/water bath and, after 10 min, 15 mmol of dicyclohexylcarbodiimide (DCC) were added under an argon atmosphere. The mixture was stirred overnight at room temperature, the salts were filtered off and the solvent was evaporated. The crude product was purified by flash chromatography using a mixture of hexanes/ethyl acetate (7/1) as eluant.

3.1.3.1. *(1R)-1-Methylheptyl 4-benzyloxybenzoate.* See ref. [1].

3.1.3.2. *(1R)-1-Methyloctyl 4-benzyloxybenzoate.* Yield 56% of a yellow oil, R_f 0.72 (80/20 hexanes/ethyl acetate). ^{1}H NMR (300 MHz, $CDCl_3$): ∂ 0.85 (t, $J=6.9$ Hz, 3H), 1.24 (m, 10H), 1.30 (d, $J=6$ Hz, 3H), 1.57 (m, 1H), 1.69 (m, 1H), 5.1 (m, 3H), 6.97 (d, $J=9$ Hz, 2H), 7.24–7.43 (m, 5H), 7.98 (d, $J=9$ Hz, 2H). ^{13}C NMR (300 MHz, $CDCl_3$): ∂ 14.1, 20.1, 22.6, 25.4, 29.2, 29.5, 31.8, 36.1, 70.0, 71.3, 114.3, 123.6, 127.4, 128.2, 128.7, 131.5, 136.3, 162.3, 165.9. IR(Nujol): ν 1710, 1274, 1250, 1167, 1103 cm^{-1}.

3.1.3.3. *Synthesis of (1S)-1-methylpentadecyl 4-benzyloxybenzoate,* ***1 (n=14).*** A mixture of 12.9 mmol of 4-benzyloxybenzoic acid, 12.9 mmol of (2*R*)-2-hexadecanol and 12.9 mmol of triphenylphosphine (TPP) in 100 ml of dry diethyl ether was stirred for 30 min at 0°C under an argon atmosphere. 16.1 mmol of diethyl azodicarboxylate (DEAD) were added dropwise by syringe. The mixture was stirred for 24 h at room temperature. 10 drops of water were added and the mixture was stirred for 1 h. The solvent was evaporated and the residue stirred in a mixture of hexanes/ethyl acetate (7/3). The mixture was filtered through Celite® and the solvent evaporated. The crude product was purified by flash chromatography using a mixture of hexanes/toluene (1/1) as eluant. Yield 65% of a white solid, m.p. 45°C, R_f 0.76 (80/20 hexanes/ethyl acetate). ^{1}H NMR (300 MHz, $CDCl_3$): ∂ 0.87 (t, $J=6.9$ Hz, 3H), 1.24 (m, 24H), 1.30 (d, $J=6.3$ Hz, 3H), 1.59 (m, 1H), 1.69 (m, 1H), 5.1 (m, 3H), 6.97 (d, $J=8.7$ Hz, 2H), 7.32–7.43 (m, 5H), 7.98 (d, $J=9$ Hz, 2H). ^{13}C NMR (300 MHz, $CDCl_3$): ∂ 14.1, 20.1, 22.7, 25.4, 29.3, 29.5, 29.6, 29.7, 31.9, 36.1, 70.0, 71.3, 114.3, 123.6, 127.4, 128.1, 128.6, 131.5, 136.3, 162.3, 165.9. IR (Nujol): ν 1711, 1275, 1250, 1167, 1104 cm^{-1}.

3.1.4. *General procedure for synthesis of 1-methylalkyl 4-hydroxybenzoates,* ***2***

To a mixture of 7.34 mmol of 1-methylalkyl 4-benzyloxybenzoate, were added 30 ml of cyclohexene and 60 ml of ethanol under an argon atmosphere. 0.5 g of $Pd(OH)_2$/C (20%) was then added in small portions. The mixture was heated at reflux for 24 h; it was then filtered through a pad of Celite® and the solvent evaporated. The crude product was purified by flash chromatography using dichloromethane as eluent.

3.1.4.1. *(1R)-1-Methyheptyl 4-hydroxybenzoate.* See ref. [1].

3.1.4.2. *(1R)-1-Methyloctyl 4-hydroxybenzoate.* Yield 98% of an orange oil, R_f 0.42 (80/20 hexanes/ethyl acetate). ^{1}H NMR (300 MHz, $CDCl_3$): ∂ 0.84 (t, $J=6.9$ Hz, 3H), 1.24 (m, 10H), 1.30 (d, $J=6.3$ Hz, 3H), 5.1 (m, 1H), 6.84 (d, $J=8.7$ Hz, 2H), 7.93 (d, $J=8.7$ Hz, 2H). ^{13}C NMR (300 MHz, $CDCl_3$): ∂ 14.1, 20.1, 22.6, 25.4, 29.2, 29.4, 31.8, 36.1, 71.6, 115.1, 122.4, 131.8, 160.4, 167.0. IR (Nujol): ν 3351, 1708, 1679, 1279, 1232, 1165, 1114 cm^{-1}.

3.1.4.3. *(1S)-1-Methylpentadecyl 4-hydroxybenzoate.* Yield 94% of a white solid, R_f 0.46 (80/20 hexanes/ethyl acetate), m.p. 63°C. ^{1}H NMR (300 MHz, $CDCl_3$): ∂ 0.86 (t, $J=6.9$ Hz, 3H), 1.23 (m, 24H), 1.31 (d,

$J=6.3$ Hz, 3H), 1.58 (m, 1H), 1.69 (m, 1H), 5.11 (m, 1H), 6.54 (broad, 1H), 6.87 (d, $J=8.7$ Hz, 2H), 7.93 (d, $J=8.7$ Hz, 2H). ^{13}C NMR: ∂ 14.4, 20.3, 22.9, 25.7, 29.6, 29.8, 29.9, 30.0, 32.2, 36.3, 72.1, 115.5, 123.2, 132.1, 160.5, 166. IR (Nujol): ν 3373 (w), 1683, 1276, 1230, 1161, 1107 cm^{-1}.

3.1.5. *General procedure for synthesis of 4-(1-methylalkoxycarbonyl)phenyl 4-nitrobenzoate,* ***3***

The esterification of *p*-nitrobenzoic acid with the corresponding phenols was carried out with DCC and DMAP in dichloromethane, in a similar way to that described for (1*R*)-1-methylheptyl 4-benzyloxybenzoate. The reaction gave better yields than in the case of aliphatic alcohols and was carried out at room temperature. The crude product was purified by flash chromatography on silica gel using a mixture of hexanes/ethyl acetate (1/7) as eluant.

3.1.5.1. *4-[(1R)-1-Methyheptyloxycarbonyl]phenyl 4-nitrobenzoate.* See ref. [1].

3.1.5.2. *4-[(1R)-1-Methyloctyloxycarbonyl]phenyl 4-nitrobenzoate.* Yield 61% of a white solid, R_f 0.62 (80/20 hexanes/ethyl acetate), m.p. 42°C. ^{1}H NMR (300 MHz, $CDCl_3$): ∂ 0.85 (t, $J=6.3$ Hz, 3H), 1.25 (m, 10H), 1.32 (d, $J=6.3$ Hz, 3H), 1.59 (m, 1H), 1.7 (m, 1H), 5.15 (m, 1H), 7.29 (d, $J=8.7$ Hz, 2H), 8.13 (d, $J=8.7$ Hz, 2H), 8.36 (s, 4H). ^{13}C NMR (300 MHz, $CDCl_3$): ∂ 14.0, 20.0, 22.6, 25.4, 29.2, 29.4, 31.8, 36.0, 72.1, 121.4, 123.8, 129.2, 131.3, 131.4, 134.5, 151.1, 153.9, 162.8, 165.2. IR (Nujol): ν 1746, 1714, 1521, 1346, 1256, 1208, 1160, 1073 cm^{-1}.

3.1.5.3. *4-[(1S)-1-methypentadecyloxycarbonyl]phenyl 4-nitrobenzoate.* Yield 67% of a white solid, R_f 0.68 (80/20 hexanes/ethyl acetate), m.p. 65°C. ^{1}H NMR (300 MHz, $CDCl_3$): ∂ 0.84 (t, $J=6.3$ Hz, 3H), 1.22 (m, 24H), 1.32 (d, $J=6.3$ Hz, 3H), 1.59 (m, 1H), 1.71 (m, 1H), 5.15 (m, 1H), 7.29 (d, $J=8.7$ Hz, 2H), 8.12 (d, $J=8.7$ Hz, 2H), 8.35 (s, 4H). ^{13}C NMR (300 MHz, $CDCl_3$): ∂ 14.0, 20.1, 22.7, 25.4, 29.0, 29.4, 29.5, 29.6, 29.7, 31.9, 36.0, 72.1, 121.4, 123.8, 129.2, 131.3, 131.4, 134.5, 151.0. 153.8, 162.9, 165.3. IR (Nujol): ν 1745, 1713, 1524, 1349, 1257, 1207, 1161, 1073 cm^{-1}.

3.1.6. *General procedure for synthesis of 4-(1-methylalkoxycarbonyl)phenyl 4-aminobenzoates,* ***4***

To a solution of 1 mmol of the corresponding 4-(1-methylalkoxycarbonyl)phenyl 4-nitrobenzoate (obtained in the previous step) in 16 ml of a mixture of cyclohexene/absolute ethanol (1/1), was added 68 mg of $Pd(OH)_2/C$ (20%) in small portions under an argon atmosphere. The suspension was heated under reflux for 90 min. The mixture was cooled, filtered through a pad of Celite® and, in most cases, the crude product was used in the next reaction without further purification. The pure compound was obtained by recrystallization from ethanol/water (3/1).

3.1.6.1. *4-[(1R)-1-Methyheptyloxycarbonyl]phenyl 4-aminobenzoate.* Yield 98% of a white solid, R_f 0.17 (80/20 hexanes/ethyl acetate), m.p. 77°C. ^{1}H NMR (300 MHz, $CDCl_3$): ∂ 0.85 (t, $J=7.1$ Hz, 3H), 1.26 (m, 8H), 1.32 (t, $J=6.2$ Hz, 2H), 1.59 (m, 1H), 1.66 (m, 1H), 4.16 (s, 2H) 5.13 (m, 1H), 6.67 (d, $J=8.8$ Hz, 2H), 7.24 (d, $J=8.8$ Hz, 2H), 7.98 (d, $J=8.8$ Hz, 2H), 8.08 (d, $J=8.8$ Hz, 2H). ^{13}C NMR (300 MHz, $CDCl_3$): ∂ 14.1, 20.1, 22.6, 25.4, 29.1, 31.7, 36.1, 71.9, 113.8, 118.1, 121.8, 128.1, 131.0, 132.5, 151.8, 154.9, 164.7, 165.6. IR (Nujol): ν 3460, 3362, 3224, 1703, 1279, 1205, 1171, 1064 cm^{-1}.

3.1.6.2. *4-[(1R)-1-Methyloctyloxycarbonyl]phenyl 4-aminobenzoate.* Yield 96% of a white solid, R_f 0.17 (80/20 hexanes/ethyl acetate). m.p. 74°C. ^{1}H NMR (300 MHz, $CDCl_3$): ∂ 0.85 (t, $J=6.3$ Hz, 3H), 1.25 (m, 10H), 1.31 (t, $J=6.3$ Hz, 3H), 1.59 (m, 1H), 1.68 (m, 1H), 4.19 (s, 2H) 5.13 (m, 1H), 6.66 (d, $J=8.1$ Hz, 2H), 7.24 (d, $J=8.1$ Hz, 2H), 7.97 (d, $J=8.1$ Hz, 2H), 8.07 (d, $J=8.1$ Hz, 2H). ^{13}C NMR (300 MHz, $CDCl_3$): ∂ 14.1, 20.1, 22.6, 25.4, 29.2, 29.4, 31.8, 36.0, 71.9, 113.8, 118.1, 121.8, 128.1, 131.0, 132.5, 151.8, 154.9, 164.7, 165.6. IR (Nujol): ν 3416, 3333, 3230, 1703, 1276, 1204, 1171, 1066 cm^{-1}.

3.1.6.3. *4-[(1S)-1-Methypentadecyloxycarbonyl]phenyl 4-aminobenzoate.* Yield 98% of a white solid, R_f 0.22 (80/20 hexanes/ethyl acetate), m.p. 94°C. ^{1}H NMR (300 MHz, $CDCl_3$): ∂ 0.86 (t, $J=5.7$ Hz, 3H), 1.23 (m, 24H), 1.32 (d, $J=5.7$ Hz, 3H), 1.58 (m, 1H), 1.69 (m, 1H), 4.18 (s broad, 2H), 5.1 (m, 1H), 6.68 (d, $J=7.8$ Hz, 2H), 7.25 (d, $J=7.8$ Hz, 2H), 7.99 (d, $J=8.1$ Hz, 2H), 8.08 (d, $J=8.1$ Hz, 2H). ^{13}C NMR (300 MHz, $CDCl_3$): ∂ 14.1, 20.1, 22.7, 25.4, 29.4, 29.5, 29.5, 29.6, 29.7, 31.9, 36.1, 71.9, 113.9, 118.3, 121.8, 128.2, 131.0, 132.5, 151.7, 154.8, 157.5, 164.7, 165.6. IR (Nujol): ν 3416, 3332, 3229, 1704, 1276, 1204, 1173, 1067 cm^{-1}.

3.1.7. *Synthesis of alkoxybenzaldehydes,* ***5***

3.1.7.1. *Synthesis of 4-octyloxy-2-hydroxybenzaldehyde.* See ref. [1].

3.1.7.2. *Synthesis of 4-(1H,1H,2H,2H-perfluorooctyloxy)-2-hydroxybenzaldehyde.* A mixture of 21.3 mmol of 2,4-dihydroxybenzaldehyde, 20.2 mmol

of 1H,1H,2H,2H-perfluorooctanol, 20.2 mmol of triphenylphosphine (TPP) in 130 ml of dry diethyl ether was stirred for 30 min at 0°C under an argon atmosphere. 23.6 mmol of diethyl azodicarboxylate (DEAD) were added dropwise by syringe. The mixture was stirred for 20 h at room temperature; six drops of water were added and the mixture was stirred for a further 1 h. The solvent was evaporated and the residue stirred in 20 ml of a mixture of hexanes/ethyl acetate (7/3). The mixture was filtered through a pad of Celite® and the solvent removed under reduced pressure. The crude product was purified by flash chromatography using a mixture of hexanes/ethyl acetate (5/1) as eluent and, finally, the compound was recrystallized from hexanes. Yield 22% of white needles, R_f 0.54 (80/20 hexanes/ethyl acetate), m.p. 72°C. ^{1}H NMR (300 MHz, $CDCl_3$): ∂ 2.63 (m, 2H), 4.29 (t, $J=6.1$ Hz, 2H), 6.41 (d, $J=2.1$ Hz, 1H), 6.52 (dd, $J=2.1$ Hz, $J=8.4$ Hz, 1H), 7.43 (d, $J=8.4$ Hz, 1H), 9.7 (s, 1H), 11.4 (s, 1H). ^{13}C NMR (300 MHz, $CDCl_3$): ∂ 30.7, 31.0, 31.3, 60.3, 101.2, 108.4, 115.6, 135.4, 164.4, 165.0, 194.5. ^{19}F NMR (300 MHz, $CDCl_3$): ∂ −81.2, −113.7, −122.3, −123.3, −123.9, −126.5. IR (Nujol): ν 3040 (br), 1647, 1627, 1228, 1209, 1187, 1140 cm^{-1}.

3.1.8. *General procedure for synthesis of 4-[(1R)-1-methylalkoxycarbonyl]phenyl N-(4′-octyloxy-2′-hydroxybenzylidene)-4-aminobenzoates,* ***L1***

A mixture of 1 mmol 4-octyloxy-2-hydroxybenzaldehyde and 1 mmol of 4-(1-methylalkoxycarbonyl)phenyl 4-aminobenzoate, **4**, and three drops of acetic acid in 10 ml of absolute ethanol was heated at reflux for 4 h. The reaction mixture was allowed to cool and was stirred at room temperature overnight. The solid was collected and recrystallized from technical ethanol.

3.1.8.1. *4-[(1R)-1-Methyloctyloxycarbonyl]phenyl N-(4′-heptyloxy-2′-hydroxybenzylidene)-4-aminobenzoate,* ***L1(H,6)***. See ref. [1].

3.1.8.2. *4-[(1R)-1-Methyloctyloxycarbonyl]phenyl N-(4′-octyloxy-2′-hydroxybenzylidene)-4-aminobenzoate,* ***L1(H,7)***. Yield 40% of a yellow solid. ^{1}H NMR (300 MHz, $CDCl_3$): ∂ 0.86 (m, 6H), 1.23–1.45 (m, 23H), 1.61 (m, 1H), 1.66–1.84 (m, 3H), 3.99 (t, $J=6.6$ Hz, 2H), 5.16 (m, 1H), 6.50 (m, 1H), 7.29 (d, $J=8.7$ Hz, 2H), 7.33 (d, $J=8.7$ Hz, 2H), 8.11 (d, $J=8.7$ Hz, 2H), 8.22 (d, $J=8.7$ Hz, 2H), 8.54 (s, 1H), 13.33 (s, 1H). ^{13}C NMR (300 MHz, $CDCl_3$): ∂ 14.0, 20.0, 22.6, 25.4, 25.9, 29.00, 29.2, 29.3, 29.4, 29.6, 31.7, 36.0, 68.3, 71.9, 101.5, 108.1, 112.7, 121.2, 121.6, 126.5, 128.5, 131.1, 131.7, 134.0, 153.4, 154.4, 163.1, 164.1, 164.2, 164.3, 165.4. IR (Nujol): ν 3433 (br), 1728, 1714, 1627, 1272 1210, 1195 cm^{-1}. Elemental analysis for $C_{37}H_{49}NO_6$: calc. C 74.12, H 8.02, N 2.27; found C 73.38, H 7.62, N 2.37%. MS (FAB+) *m/z*: (M+1) 617, 490, 352 (100%).

3.1.8.3. *4-[(1S)-1-Methylpentadecyloxycarbonyl]phenyl N-(4′-octyloxy-2′-hydroxybenzylidene)-4-aminobenzoate,* ***L1(H,14)***. Yield 20% of a yellow solid. ^{1}H NMR (300 MHz, $CDCl_3$): ∂ 0.86 (m, 6H), 1.22–1.42 (m, 37H), 1.59–1.68 (m, 1H), 1.68–1.72 (m, 3H), 4.00 (t, $J=6.6$ Hz, 2H), 5.15 (m, 1H), 6.50 (m, 1H), 7.29 (d, $J=8.7$ Hz, 2H), 7.34 (d, $J=8.4$ Hz, 2H), 8.11 (d, $J=8.7$ Hz, 2H), 8.23 (d, $J=8.4$ Hz, 2H), 8.55 (s, 1H), 13.33 (s, 1H). ^{13}C NMR (300 MHz, $CDCl_3$): ∂ 14.1, 20.1, 22.6, 22.7, 25.4, 25.9, 29.0, 29.2, 29.3, 29.4, 29.5, 29.5, 29.6, 29.7, 31.8, 31.9, 36.0, 68.4, 71.9, 101.5, 108.1, 112.7, 121.3, 121.7, 126.6, 128.6, 131.1, 131.8, 134.0, 153.5, 154.4, 163.2, 164.1, 164.2, 164.3, 165.5. IR (Nujol): ν 3600–3110 (br), 1728, 1714, 1625, 1272, 1195 cm^{-1}. Elemental analysis for $C_{45}H_{63}NO_6$: calc. C 75.70, H 8.89, N 1.96; found C 75.64, H 8.91, N 1.96%. MS (FAB+) *m/z*: (M+1) 715, 586, 490, 352 (100%).

3.1.9. *General procedure for synthesis of 4-[(1R)-1-methylalkoxycarbonyl]phenyl N-(4′-1H,1H,2H,2H-perfluorooctyloxy-2′-hydroxybenzylidene)-4-aminobenzoates,* ***L2***

A mixture of 1 mmol 4-(1*H*,1*H*,2*H*,2*H*-perfluorooctyloxy)-2-hydroxybenzaldehyde, 1 mmol of 4-(1-methylalkoxycarbonyl)phenyl 4-aminobenzoate and three drops of acetic acid in 10 ml of absolute ethanol was heated at reflux for 4 h. The reaction mixture was allowed to cool and stirred at room temperature overnight. The solid was collected and recrystallized from acetone/ethanol.

3.1.9.1. *4-[(1R)-1-Methylheptyloxycarbonyl]phenyl N-(4′-1H,1H,2H,2H-perfluorooctyloxy-2′-hydroxybenzylidene)-4-aminobenzoate,* ***L2(F,6)***. Yield 44% of a yellow solid. ^{1}H NMR (300 MHz, $CDCl_3$): ∂ 0.86 (t, $J=6$ Hz, 3H), 1.27 (m, 8H), 1.33 (d, $J=6.3$ Hz, 3H), 1.58 (m, 1H), 1.70 (m, 1H), 2.65 (m, 2H), 4.31 (t, $J=6.9$ Hz, 2H), 5.15 (m, 1H), 6.51 (m, 1H), 7.29 (d, $J=8.7$ Hz, 2H), 7.34 (d, $J=8.4$ Hz, 2H), 8.11 (d, $J=8.7$ Hz, 2H), 8.23 (d, $J=8.4$ Hz, 2H), 8.57 (s, 1H), 13.35 (s, 1H). ^{13}C NMR (300 MHz, $CDCl_3$): ∂ 14.1, 20.1, 22.6, 25.4, 29.2, 30.9, 31.5, 31.7, 36.1, 60.2, 71.9, 101.8, 107.8, 113.5, 121.3, 121.7, 127.0, 128.7, 131.2, 131.8, 134.3, 153.3, 154.5, 162.9, 163.2, 164.1, 164.2, 165.5 ^{19}F NMR (300 MHz, $CDCl_3$): ∂ −81.17, −113.69, −122.25, −123.26, −123.92, −126.53. IR (Nujol): ν 3500–3000 (br), 1725, 1708, 1622, 1245, 1208, 1194, 1134 cm^{-1}. Elemental analysis for

$C_{37}H_{34}F_{13}NO_6$: calc. C 53.18, H 4.10, N 1.68; found C 52.95, H 3.94, N 1.70%. MS (FAB+) *m/z*: (M) 836, 724, 586 (100%), 469.

3.1.9.2. *4-[(1R)-1-Methyloctyloxycarbonyl]phenyl N-(4′-1H,1H,2H,2H-perfluorooctyloxy-2′-hydroxybenzylidene)-4-aminobenzoate,* ***L2(F,7)***. Yield 40% of a yellow solid. ^{1}H NMR (300 MHz, $CDCl_3$): ∂ 0.86 (t, $J=6.9$ Hz, 3H), 1.26 (m, 10H), 1.33 (d, $J=6$ Hz, 3H), 1.58 (m, 1H), 1.69 (m, 1H), 2.65 (m, 2H), 4.32 (t, $J=6.6$ Hz, 2H), 5.15 (m, 1H), 6.52 (m, 1H), 7.29 (d, $J=8.7$ Hz, 2H), 7.34 (d, $J=8.7$ Hz, 2H), 8.12 (d, $J=8.7$ Hz, 2H), 8.24 (d, $J=8.7$ Hz, 2H), 8.58 (s, 1H), 13.35 (s, 1H). ^{13}C NMR (300 MHz, $CDCl_3$): ∂ 14.1, 20.1, 22.7, 29.2, 29.5, 30.9, 31.2, 31.5, 31.8, 36.1, 38.2, 60.2, 72.0, 101.8, 107.8, 113.5, 121.3, 121.7, 126.9, 128.7, 131.2, 131.8, 134.3, 153.3, 154.5, 162.9, 163.2, 164.1, 164.2, 164.5. ^{19}F NMR (300 MHz, $CDCl_3$): ∂ −81.30, −113.86, −122.42, −123.43, 124.09, −126. 69. IR (Nujol): 3500–3000 (br), 1725, 1709, 1629, 1242, 1210, 1195, 1137 cm^{-1}. Elemental analysis for $C_{38}H_{36}F_{13}NO_6$: calc. C 53.72, H 4.27, N 1.65; found C 53.90, H 4.17, N 1.80%. MS (FAB+) *m/z*: (M) 850, 724, 586 (100%), 469.

3.1.9.3. *4-[(1S)-1-methylpentadecyloxycarbonyl]phenyl N-(4′-1H,1H,2H,2H-perfluorooctyloxy-2′-hydroxybenzylidene)-4-aminobenzoate,* ***L2(F,14)***. Yield 16% of a yellow solid. ^{1}H NMR (300 MHz, $CDCl_3$): ∂ 0.86 (t, $J=6.6$ Hz, 3H), 1.24 (m, 24H), 1.33 (d, $J=6$ Hz, 3H), 1.60 (m, 1H), 1.70 (m, 1H), 2.65 (m, 2H), 4.3 (t, *J*: 6.9 Hz, 2H), 5.14 (m, 1H), 6.50 (d, $J=7.2$ Hz, 1H), 7.28 (d, $J=8.7$ Hz, 2H), 7.33 (d, $J=8.4$ Hz, 2H), 8.11 (d, $J=8.7$ Hz, 2H), 8.22 (d, $J=8.4$ Hz, 2H), 8.56 (s, 1H), 13.35 (s, 1H). ^{13}C NMR (300 MHz, $CDCl_3$): ∂ 14.1, 20.1, 22.7, 25.5, 29.4, 29.5, 29.6, 29.6, 29.7, 29.7, 31.1–31.9, 36.1, 60.2, 72.0, 101.8, 107.7, 121.3, 121.7, 126.8, 128.6, 131.2, 131.8, 134.3, 153.2, 154.4, 162.9, 163.2, 164.1, 164.2, 165.4. ^{19}F NMR (300 MHz, $CDCl_3$): ∂ −81.24, −113.73, −122.29, −123.31, −123.95, −126.58. IR (Nujol): *v* 3500–3000 (br), 1725, 1707, 1627, 1241, 1208, 1195, 1136 cm^{-1}. Elemental analysis for $C_{45}H_{50}F_{13}NO_6$: calc. C 57.02, H 5.32, N 1.48; found C 57.62, H 5.45, N 1.60%. MS (FAB+) *m/z*: (M) 948, 724, 586 (100%).

3.1.10. *Synthesis of the copper complex* ***L1(H,6)-Cu***

To a solution of 2 mmol of **L1(H,6)** in 20 ml of absolute ethanol, a suspension of 1 mmol of copper acetate in ethanol was added dropwise. A precipitate appeared after a few minutes, and the mixture was heated at reflux under argon for 2 h. The reaction mixture was allowed to cool and was stirred at room temperature overnight. The solid was filtered off, dissolved in dry dichloromethane, and the solution filtered through a pad of Celite®; the solvent was evaporated. The resulting solid was dried in a vacuum oven. Yield 83% of a green solid. IR(Nujol): *v* 1729, 1602, 1267 cm^{-1}. MS (FAB+) *m/z*: 1308 (M-2Na), 602, 352 (100%). Elemental analysis for $C_{74}H_{92}N_2O_{12}Cu$: calc. C 70.28, H 7.28, N 2.21; found C 70.22, H 7.08, N 2.32%.

3.1.11. *Synthesis of the vanadyl complex of 4-octyloxy-2-hydroxybenzaldehyde*

A mixture of 2 mmol of 4-octyloxy-2-hydroxybenzaldehyde, 1 mmol of vanadyl sulphate pentahydrate, 2 mmol of sodium acetate and a few drops of water in 10 ml of absolute ethanol was heated under reflux under argon for 8 h. The reaction mixture was allowed to cool and stirred at room temperature overnight. Five drops of water were added to the mixture and the green solid was filtered off, washed with water and then ether and dried in a vacuum oven. Yield 40% of a green solid. IR (Nujol): *v* 3583, 3510, 3345, 1621, 1604, 1225, 1124 cm^{-1}. Elemental analysis for $C_{30}H_{42}O_7V$: calc. C 63.71, H 7.48; found C 64.11, H 7.30%. MS (FAB+) *m/z*: 567, (M) 566, 565 (100%), 468.

3.1.12. *Synthesis of the vanadyl complex of 4-(1H,1H,2H,2H-perfluorooctyloxy)-2-hydroxybenzaldehyde*

A mixture of 1 mmol of 4-(1*H*,1*H*,2*H*,2*H*-perfluorooctyloxy)-2-hydroxybenzaldehyde, 1 mmol of sodium acetate and 0.5 mmol of vanadyl sulphate pentahydrate and a few drops of water was heated under reflux for 15 h under an inert atmosphere. The mixture was cooled and stirred at room temperature for 4 h. The solid was filtered off, washed with water and then ether and dried in a vacuum oven. Yield 47% of a pale green solid. IR (Nujol): *v* 3596, 3513, 3333, 1619, 1606, 1228, 1203, 1142 cm^{-1}. MS (FAB+) *m/z*: 1033 (M), 1017 (100%). Elemental analysis for $C_{30}H_{16}F_{26}O_7V$: calc. C 34.87, H 1.56; found C 33.20, H 1.62%.

3.1.13. *General procedure for synthesis of the vanadyl complexes* ***L1(H,6)-VO; L1(H,7)-VO; L2(F,7)-VO***

A mixture of 0.13 mmol of sodium acetate, 0.26 mmol of the vanadyl complex of 4-alkoxy-2-hydroxybenzaldehyde, **5**, and 0.26 mmol of aniline in ethanol was heated under reflux for 10 min under an inert atmosphere. The solid was filtered off and dissolved in dry toluene. This solution was filtered through a pad of Celite®, and the solvent was

evaporated. The resulting solid was dried in a vacuum oven.

3.1.13.1. ***L1(H,6)-VO***. Yield 20% of a dark green solid. IR(Nujol): *v* 1717, 1606, 1267 cm^{-1}. MS (FAB+) *m/z*: (M) 1268, 490, 352 (100%). Elemental analysis for $C_{74}H_{92}N_2O_{13}V$: calc. C 70.07, H 7.31, N 2.21; found C 69.72, H 7.48, N 2.18%.

3.1.13.2. ***L1(H,7)-VO***. Yield 22% of a dark green solid. IR(Nujol): *v* 1717, 1605, 1268 cm^{-1}. MS (FAB+) *m/z*: (M) 1296, 490, 352 (100%). Elemental analysis for $C_{76}H_{96}N_2O_{13}V$: calc. C 70.40, H 7.46, N 2.16; found C 70.23, H 7.53, N 2.14%.

3.1.13.3. ***L2(F,7)-VO.*** Yield 10% of a dark green solid. IR: *v* 1719, 1608, 1271, 1241, 1202 cm^{-1}. MS (FAB+) *m/z*: (M) 1764, 725, 587 (100%). Elemental analysis for $C_{76}H_{70}F_{26}N_2O_{13}V$: calc. C 51.74, H 4.00, N, 1.59; found C 52.66, H 4.12, N 1.94%.

3.2. *Characterization*

Infrared spectra for all the complexes were obtained by using a Perkin–Elmer 1600 (FTIR) spectrophotometer in the 400–4000 cm^{-1} spectral range. ^1H NMR spectra were recorded on a Bruker ARX 300 spectrometer in $CDCl_3$ solutions. Microanalysis was performed with a Perkin-Elmer 240 B microanalyser.

The textures of the mesophases were studied with an optical microscope (Olympus) with crossed polarizers and connected to a Linkam TMS hot stage and a Linkam THMS 600 central processor. Measurements of the transition temperatures were made using a TA2910 differential scanning calorimeter with a heating or cooling rate of 10°C min^{-1}. The apparatus was calibrated with indium (156.6°C, 28.44 J g^{-1}).

The complex permittivity was measured over 11 decades of frequency (10^{-2}–10^9 Hz) using three different measuring systems: a Schulmberger 1260 frequency response analyser accomplished with a high impedance preamplifier of a variable gain (10^{-2}–10^6); and two impedance analysers, the HP 4191A (10^2–10^7) Hz and the HP 4192A (10^6–10^9 Hz).

The spontaneous polarization was measured using the triangular wave method. In the experimental set-up the triangular wave voltage was supplied by a HP3245A function generator. The current–voltage cycles were recorded by a digital acquisition system, tech ADC488/16A. All the equipment was interfaced to a computer.

4. Conclusion

We have described the synthesis of a series of new imine-based liquid crystalline compounds which exhibit a tilted SmC* phase, and have characterized their mesomorphic and dielectric properties. As a continuation of previous work on the design of new antiferroelectric liquid crystals, the present study completes our objective of analysing and establishing the effect of different structural modifications on mesomorphism and dielectric behaviour. The complexation of some of these ligands to different metals gives rise to new ferroelectric materials, which include hydrocarbon and fluorocarbon derivatives.

This work was supported by the C.I.C.Y.T (MAT 2003-07806-CO2) and FEDER founding (UE and DGA).

References

[1] López, D., Piñol, R., Ros, M. B., Serrano, J. L., Sierra, T., and de la Fuente, M. R., 2004, *J. Mater. Chem.*, **14,** 1117.
[2] For studies concerning achiral Schiff's base complexes see: Serrano, J. L. and Sierra, T., 1996, in *Metallomesogens. Synthesis, Properties and Applications* (Weinheim: Wiley-VCH), Chap. 3.
[3] Goodby, J. W., Patel, J. S., and Chin, E., 1992, *J. mater. Chem.*, **2,** 197.
[4] Fukuda, A., Takanishi, Y., Isozaki, T., Ishikawa, K., and Takezoe, H., 1994, *J. mater. Chem.*, **4,** 997.
[5] Cumming, W. J., and Gaudiana, R. A., 1996, *Liq. Cryst.*, **20,** 283.
[6] (*a*) Liu, H., and Nohira, H., 1996, *Liq. Cryst*., **20,** 581; (*b*) Liu, H., and Nohira, H., 1997, *Liq. Cryst*., **22,** 217; (*c*) Liu, H., and Nohira, H., 1998, *Liq. Cryst*., **24,** 719.
[7] Heppke, G., Kleineberg, P., and Lötzsch, D., 1993, *Liq. Cryst.*, **14,** 67.
[8] Pérez-Jubindo, M. A., Tello, M. J., and Fernández, J., 1981, *J. Phys. D*, **14,** 2305.
[9] Mitsunobu, O., 1981, *Synthesis*, **1,** 1.
[10] Taffin de Givenchy, E., Guittard, F., Bracon, F., and Cambon, A., 1999, *Liq. Cryst.*, **26,** 1163.
[11] For a review on fluorinated liquid crystals see: Guittard, F., Taffin de Givenchy, E., Geribaldi, S., and Cambon, A., 1999, *J. fluor. Chem*., **100**, 85, and references therein.
[12] Nguyen, H. T., Rouillon, J. C., Babeau, A., Marcerou, J. P., Sigaud, G., Cotrait, M., and Allouchi, H., 1999, *Liq. Cryst.*, **26,** 1007.
[13] (*a*) Drzewinski, W., Czuprynski, K., Dabrowski, R., and Neubert, M., 1999, *Mol. Cryst. liq. Cryst*., **328,** 401; (*b*) Dabrowski, R., 2000, *Ferroelectrics*, **243,** 1.
[14] Faye, V., Rouillon, J. C., Nguyen, H. T., Détré, L., Laux, V., and Isaert, N., 1998, *Liq. Cryst.*, **24,** 747.
[15] (*a*) Marcos, M., Serrano, J. L., Sierra, T., and Giménez, M. J., 1992, *Angew. Chem. int. Ed. Eng*., **31,** 1471; (*b*) Iglesias, R., Marcos, M., Serrano, J. L., Sierra, T., and Pérez-Jubindo, M. A., 1996, *Chem. Mater*., **8,** 2611.